New Diamond and Frontier Carbon Technology
Vol. 15, No. 2 2005
MYU Tokyo

NDFCT 476

Carbon Nanoballoon Produced by Thermal Treatment of Arc Soot

Guochun Xu, Hiroaki Niwa, Toyohiro Imaizumi,
Hirofumi Takikawa*, Tateki Sakakibara, Kazuo Yoshikawa[1],
Akira Kondo[1] and Shigeo Itoh[2]

Department of Electrical and Electronic Engineering, Toyohashi University of Technology,
1-1 Hibarigaoka, Tempaku, Toyohashi, Aichi 441-8580, Japan
[1]Fuji Research Laboratory, Tokai Carbon Co., Ltd., Shizuoka, Japan
[2]Product Development Center, Futaba Co., Chiba, Japan

(Received 1 October 2004; accepted 29 November 2004)

Key words: carbon nanoballoon (CNB), arc discharge, arc soot, carbon nanohorn (CNH), thermal treatment, characterization

A novel form of balloonlike carbon material (carbon nanoballoon abbreviated CNB), with a diameter of 40 ± 15 nm and a shell thickness of 10 nm, was found after thermal treatment of arc soot at more than 2400°C. The arc soot was prepared by arc discharge between a pair of pure graphite rods under nitrogen (N_2) atmosphere. The characterization of the CNB by field-emission scanning electron microscopy (FE-SEM), transmission electron microscopy (TEM) and Raman spectroscopy shows that the CNB is highly graphitized carbon, and the CNB exists in forms of individual deformed balls and ball aggregates. The thermal growth of the CNB from the arc soot was followed by TEM observation. The methods for the introduction of pinholes and for the thickness control of the balloon shells were also investigated for the further application of this nanoballoon-like material.

*Corresponding author: e-mail: takikawa@eee.tut.ac.jp

1. Introduction

Since the discovery of fullerene in 1985,[1] a number of novel carbon nanostructures, such as carbon nanotubes (CNTs),[2] carbon onions,[3] cone-shaped graphitic structures,[4] carbon microtrees,[5] and other nanoscale graphitic particles,[6] have been added to the family of carbon nanomaterials.

These nanomaterials with sizes in the domain between the quantum effects of molecules and the bulk properties of materials have numerous promising properties, including unique mechanical and electrical behaviors[7–9] and are under investigation for a wide range of practical applications such as field-emission displays,[10] hydrogen storage,[11,12] nanocomposites,[13,14] and fuel cells.[15,16]

There are various methods of fabricating carbon nanomaterials such as electric arc discharge, laser ablation, chemical vapor deposition, electrolysis, polymerization,[17] and pyrolysis. The arc discharge method was first developed in 1990 by Kräschmer *et al.*[18] for fullerene production, and is still the most popular method used in the synthesis of nanomaterials such as fullerenes and CNTs.[19] In this method, the DC arc discharge is generated between two graphite rod electrodes. The anode is evaporated violently and produces arc soot. Multiwalled carbon nanotubes (MWCNTs) were obtained from the cathode deposit.[20] Arc soot has also been found containing nanomaterials such as fullerenes, CNTs, and nanohorns (CNHs).[21–23]

We have developed the torch arc method[24] using a welding arc torch for syntheses of MWCNTs and single-walled carbon nanotubes (SWCNTs) in open air. We also found that CNHs coexisted in the arc soot. We then developed the cavity arc jet method to increase CNH yield.[25] We are among the first to demonstrate that CNHs were able to be synthesized by arc discharge, instead of laser ablation.[26]

Here, we report a novel carbon material obtained by the thermal treatment of the carbon soot produced by arc discharge of graphite electrodes under nitrogen (N_2) gas atmosphere. The novel carbon material was characterized by techniques including field-emission scanning electron microscopy (FE-SEM), transmission electron microscopy (TEM) and Raman spectroscopy. It was found that the novel materials were balloonlike highly graphitized carbon with a diameter in the range of 30–100 nm, and a shell thickness from 3.5–5.5 nm. This balloonlike graphitic carbon is named carbon nanoballoon (CNB) in this paper. We also report a method of generating pinholes on the CNB for further application as a nanosized container as well as an absorbent.

2. Experimental

The arc soot was prepared in a DC arc discharge reactor with graphite electrodes. The experiment was carried out at a current of 150 A through the two electrodes with a gap of approximately 3–5 mm. The initial pressure was adjusted to 80 kPa with N_2 gas, and the processing time was 1 to 10 min. The apparatus was described previously.[24] After arc discharge was finished, the soot on the electrodes and that on the cooled chamber were collected. We call the collected soot arc soot in this paper.

The arc soot was thermally treated in argon (Ar) gas up to 2800°C to increase its degree of crystallinity. Vacant particles with graphite shells (CNBs) were found after the thermal

treatment of the arc soot.

To further explore the possible application of the CNBs, they were treated in air at approximately 650°C. Pinholes were found formed at the joints of the graphite sheets of the balloon shells.

All of the samples collected were first observed by FE-SEM (S-4500II, Hitachi, Japan) and were further characterized by TEM (JEM-100S, JEOL, Japan) and Raman spectroscopy (RS-1000, JASCO, Japan).

3. Results and Discussion

3.1 *Arc soot*

The arc soot collected from the cold wall of the reactor was observed by FE-SEM. As shown in Fig. 1, the image of the typical arc soot reveals that unique ball-like materials are present in large quantities. These ball-like materials are present both as individual spheres and as the aggregates of spheres. The sizes of the spheres were measured in several visual fields, and the average diameter of the spheres is approximately 35 nm with a standard deviation of 10 nm.

When these ball-like materials are observed by TEM, as shown in Fig. 2, they appear to be in several forms such as graphite spheres with a horned surface (a), graphite spheres with a smooth surface (b), amorphous spheres (c), and some structures other than spheres (d). All these forms appear in fairly low densities.

In the first-order Raman spectrum of the arc soot, as shown in Fig. 3, there appear two sharp peaks at approximately 1590 and 1335 cm^{-1}, which are respectively identified as the *G* peak of crystalline graphite and the *D* peak induced by the disordered structures due to their finite crystalline size.[27,28] The comparable intensities of the two peaks indicated that the arc soot consists of significant quantities of both graphitized and amorphous structures. The second-order Raman spectrum is also shown in Fig. 3. The peak at approximately 2705 cm^{-1} (*G'*) is a crystalline-graphite-related peak, and the peak at 2944 cm^{-1} is attributed to the combination of the *D* and *G* peaks. This result, with the TEM observation, demonstrates that the arc soot is a mixture of graphitic carbon and amorphous carbon.

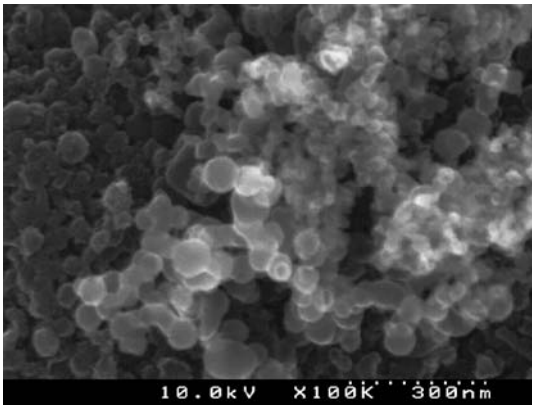

Fig. 1. FE-SEM image of as-prepared arc soot.

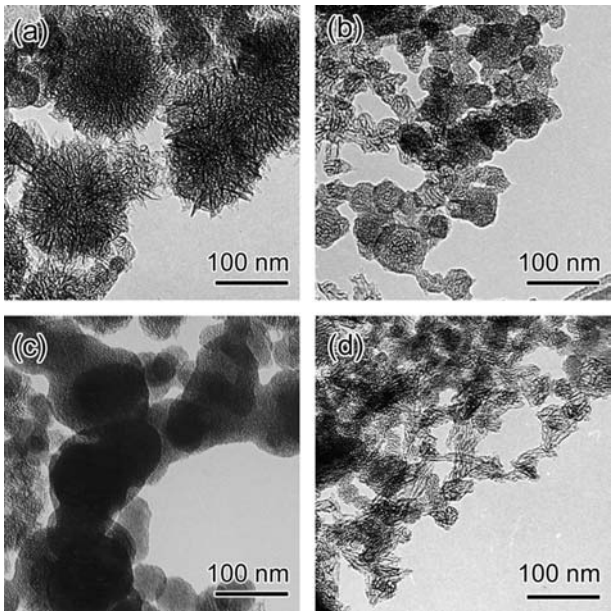

Fig. 2. TEM images of as-prepared arc soot. (a) Graphite spheres with horned surface, (b) graphite spheres without horned surface, (c) amorphous spheres, and (d) structures other than spheres.

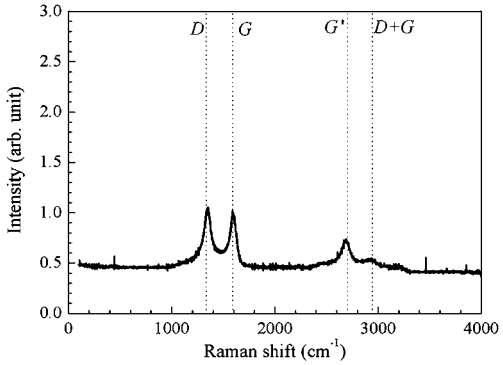

Fig. 3. Raman spectra of as-prepared arc soot.

3.2 *Carbon Nanoballoon (CNB)*

The arc soot was annealed in argon atmosphere for 30 min at 1600, 2000, 2400, and 2800°C. Figure 4 shows SEM images of the thermal-treated arc soot at 2800°C. Compared with the as-prepared arc soot, the particles of the CNBs become polygonal and their average size is 39 nm with a standard deviation of 24 nm. The distributions of the particle sizes of the arc soot and the thermal-treated samples are shown in Fig. 5. The distribution center shifts a little to the lower side and the distribution becomes broader at the high side. That

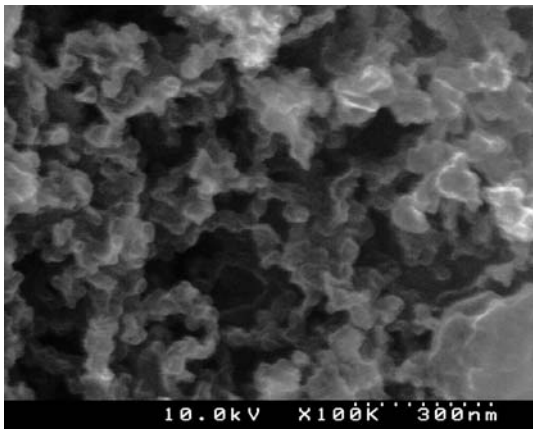

Fig. 4. FE-SEM image of CNBs from arc soot heated at 2800°C in Ar.

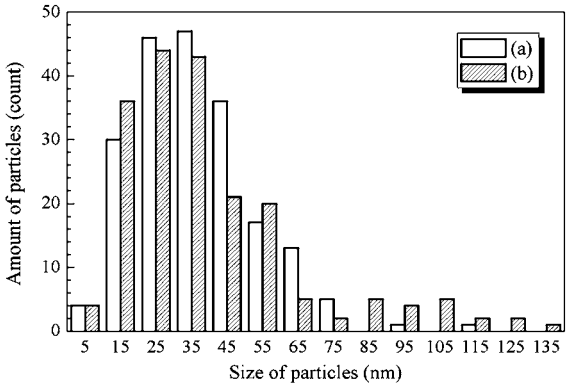

Fig. 5. Size distributions of first-order particles observed by FE-SEM for as-prepared arc soot (a) and CNBs (b) from arc soot heated at 2800°C in Ar.

is, most of the particles suffered from very small shrinkage during the thermal treatment, and a small number of adjacent particles fused with each other to form larger balloons.

Figures 6(a)–6(d) show TEM images of the arc soot annealed in argon atmosphere for 30 min at 1600, 2000, 2400 and 2800°C, respectively. The graphitic shells are formed from the outsides of the spherical arc soot, and the thickness of the shells increases gradually with treatment temperature. Because there are no obvious size changes in the spherical structure of the arc soot, the carbon supply for the growth of the shells originates from the migration of carbon inside the shells. From the increased contrast of the shells against the central parts in the TEM image, we come to the conclusion that the graphitized arc soot is an aggregate of the vacant spheres (CNBs). Since the graphite shells tend to spread out in one plane, the CNB is not a vacant ball with a perfect spherical surface, but is one with a curved surface of connected graphite sheets.

Figure 7 shows the Raman spectra of the CNB. Compared with that of the as-prepared arc soot in Fig. 3, the relative intensities of the *G* and *G'* peaks increase with annealing

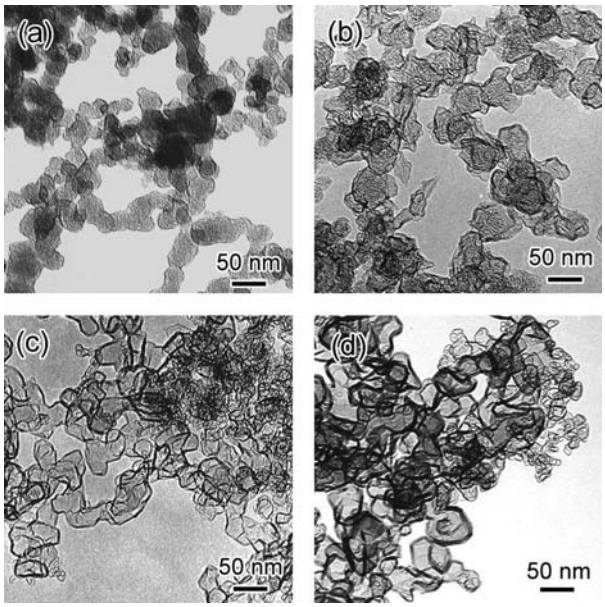

Fig. 6. TEM images of arc soot heated in Ar for 30 min at (a) 1600, (b) 2000, (c) 2400 and (d) 2800°C.

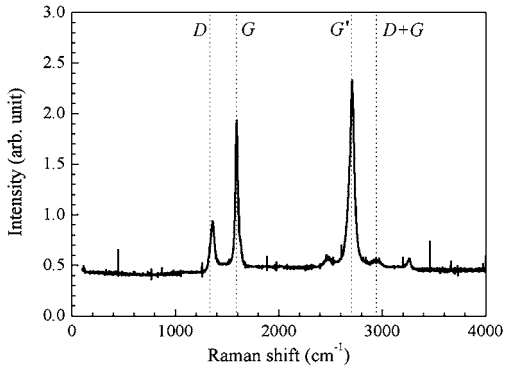

Fig. 7. Raman spectra of CNB formed from arc soot annealed in Ar at 2800°C.

temperature. This implies that the degree of graphite crystallinity in the arc soot increases after annealing at a higher temperature. This is again in agreement with the TEM observation.

We also treated Ketjenblack and carbon black in the same way. The CNB was found to be produced from Ketjenblack, but not from carbon black. This fact suggests that the density of the raw materials play an important role in the formation of the CNBs. Detailed studies on other carbon materials are still being carried out by our group.

3.3 *Pinhole Generation*

The as-prepared CNBs, with a high degree of graphite crystallinity as well as a low volume density, is expected to be a material with high electric conductivity per unit volume, and thus is a promising filler for high-performance composites. Considering the application of the CNB as a tiny container or absorbent, we need a way to open and close the balloon whenever necessary.

CNBs were oxidized in air for 15 min at 600, 625 and 650°C. Figure 8 shows TEM images of the oxidized CNBs. The graphite shells are peeled off layer by layer, by gradually increasing the temperature of the atmosphere. The average thicknesses are 9.3, 4.3, and 2.0 nm for the CNBs oxidized for 15 min at 600, 625 and 650°C, respectively. Figure 9 shows an image of the pinhole, which was taken by chance because it is difficult to find such tiny pinholes in wider observation area by TEM. The pinholes are found to be generated during the oxidation process and are mainly located at the connection points of the graphite sheets of the balloon shells.

Figure 10 graphs the changes in the surface area and weight of the CNBs with increasing oxidation temperature. When the CNBs are heated in air for one hour, the CNBs lose weight slowly with increasing temperature up to 550°C, and burn quickly when the temperature is

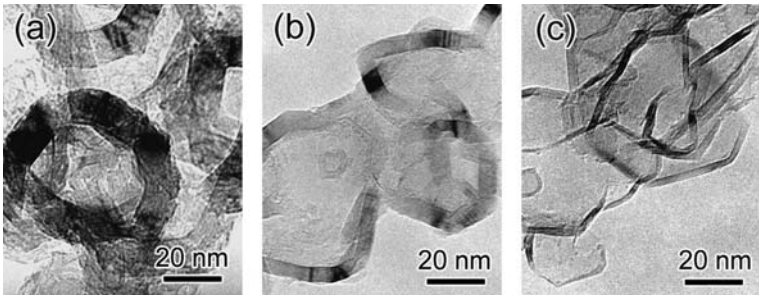

Fig. 8. TEM images of CNB oxidized in air for 15 min at (a) 600, (b) 625 and (c) 650°C.

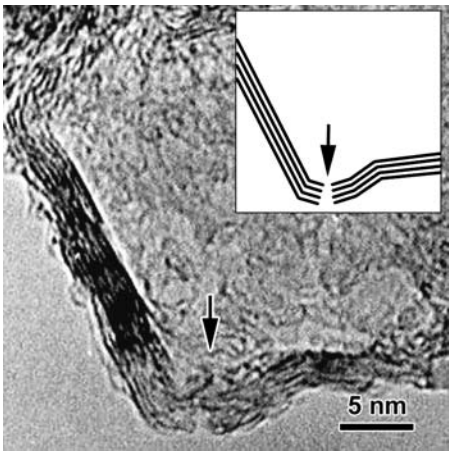

Fig. 9. Magnified TEM image of CNB oxidized at 625°C for 15 min in air. The insert illustrates the pinhole formed at a connection point of the graphite sheets of the balloon shell.

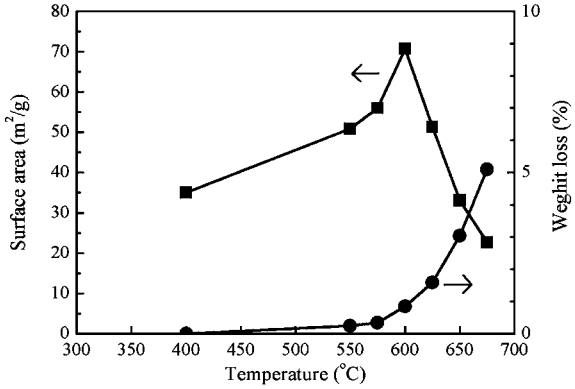

Fig. 10. Surface area changes and weight loss of CNB after oxidation in air for 1 h at different temperatures. (●) Weight loss and (■) change in surface area.

over 625°C. At the same time, the surface area of the CNBs increases along with the weight loss and reaches a maximum of approximately double the initial surface area of the CNBs at the oxidation temperature of 600°C for 1 h oxidation. When we rationally suppose that the adsorption occurred on the graphite surface, the doubled surface area implies the full opening of the balloon. The over-oxidation burns out the graphite shell and causes the drastic weight loss as well as the change in the surface area of the CNBs.

When oxidized for a shorter time, the peak of the surface area shifts to a higher temperature. For example, when the oxidation time is 15 min, the peak of the surface area appears at 625°C.

4. Conclusions

CNBs were fabricated through thermal annealing of the arc soot prepared by arc discharge between graphite electrodes in N_2 gas. The size of the carbon balloon, depending on the size of the precursor in the arc soot, has an average diameter of 40 nm, and an average shell thickness of 10 nm. The shells of the CNBs are initially formed through the graphitization of the surface carbons on the spherical precursors of the arc soot, and become thicker through the migration of the inner carbons onto the inner side of the shell. Finally, the CNBs are formed as vacant balls with highly graphitized carbon shells when the annealing temperature is over 2400°C. The graphitic shells are linked planar graphite sheets rather than perfect spherical surfaces. The joint points can be opened as pinholes by mild oxidation. The thermal oxidation of the CNBs also causes the peel off of the graphite shells, the shell thickness can be adjusted down to 2 nm. The best oxidation condition is at 625°C for 15 min. The weight loss is below 5% while the surface area doubles under this condition.

The CNB, with a highly graphitized shell and vacant inner space, has a high electric conductivity per unit volume, and is a promising filler for high-performance composites. The CNB with pinholes can be expected to be used as a tiny container for a controlled drag delivery system and as a nanosized absorbent for storage of gas, liquid and solids. We also found that CNB can be generated from other carbon precursors such as Ketjenblack in the same process.

Acknowledgments

This work was partly supported by the Excellent Research Project of the Research Center for Future Technology, Toyohashi University of Technology, by the research project of the Venture Business Laboratory, Toyohashi University of Technology, by the 21st Century COE Program "Intelligent Human Sensing" from the Ministry of Education, Culture, Sports, Science and Technology, and by a Grant-in-Aid from The Japan Society for the Promotion of Science.

References

1) H. W. Kroto, J. R. Heath, S. C. O'Brien, R. F. Curl and R. E. Smalley: Nature **318** (1985) 162.
2) S. Iijima: Nature **354** (1991) 56.
3) D. Ugarte: Nature **359** (1992) 707.
4) A. Krishnan, E. Dujardin, M. M. J. Treacy, J. Hugdahl, S. Lynum and T. W. Ebbesen: Nature **388** (1997) 451.
5) P. M. Ajayan, J. M. Nugent, R. W. Siegel, B. Wei and Ph. Kohler-Redlich: Nature **404** (2000) 243.
6) F. Kokai, A. Koshio, D. Kasuya, K. Hirahara, K. Takahashi, A. Nakayama, M. Ishihara, Y. Koga and S. Iijima: Carbon **42** (2004) 2515.
7) M. M. J. Treacy, T. W. Ebbesen and J. M. Gibson: Nature **381** (1996) 678.
8) E. W. Wong, P. E. Sheehan and C. M. Lieber: Science **277** (1997) 1971.
9) S. Frank, P. Poncharal, Z. L. Wang and W. A. de Heer: Science **280** (1998) 1744.
10) C. J. Lee, T. J. Lee and J. Park: Chem. Phys. Lett. **340** (2001) 413.
11) A. Chambers, C. Park, R. T. K. Baker and N. M. Rodriguez: J. Phys. Chem. B **102** (1998) 4253.
12) C. Park, P. E. Anderson, A. Chambers, C. D. Tan, R. Hidalgo and N. M. Rodriguez: J. Phys. Chem. B **103** (1999) 10572.
13) R. Andrews, D. Jacques, A. M. Rao, T. Rantell, F. Derbyshire, Y. Chen, J. Chen and R. C. Haddon: Appl. Phys. Lett. **75** (1999) 1329.
14) J. Sandler, M. S. P. Shaffer, T. Prasse, W. Bauhofer, K. Schulte and A. H. Windle: Polymer **40** (1999) 5967.
15) C. A. Bessel, K. Laubernds, N. M. Rodriguez and R. T. K. Baker: J. Phys. Chem. B **105** (2001) 1115.
16) E. S. Steigerwalt, G. A. Deluga, D. E. Cliffel and C. M. Lukehart: J. Phys. Chem. B **105** (2001) 8097.
17) D. Hulicova and A. Oya: Carbon **41** (2003) 1443.
18) W. Krätschmer, L. D. Lamb, K. Fostiropoulos and D. R. Huffman: Nature **347** (1990) 354.
19) J. N. Coleman, R. C. Barklie and W. J. Blau: Carbon **40** (2002) 923.
20) H. Takikawa, M. Kato, Y. Hibi, T. Sakakibara, T. Tahara and S. Itoh: Physica B **323** (2002) 287.
21) P. J. F. Harris, S. C. Tsang, J. B. Claridge and M. L. H. Green: J. Chem. Soc., Faraday Trans. **90** (1994) 2799.
22) S. Iijima, T. Wakabayashi and Y. Achiba: J. Phys. Chem. **100** (1996) 5839.
23) H. Takikawa, M. Ikeda, K. Hirahara, Y. Hibi, Y. Tao, P. A. Ruiz, Jr., T. Sakakibara, S. Itoh and S. Iijima: Physica B **323** (2002) 277.
24) M. Ikeda, H. Takikawa, T. Tahara, Y. Fujimura, M. Kato, K. Tanaka, S. Itoh and T. Sakakibara: Jpn. J. Appl. Phys. **41** (2002) L 852.
25) S. Iijima, M. Yudasaka, R. Yamada, S. Bandow, K. Suenaga, F. Kokai and K. Takahashi: Chem. Phys. Lett. **309** (1999) 165.
26) H. Takikawa, M. Imamura, M. Kouchi and T. Sakakibara: Fullerene Sci. Technol. **6** (1998) 339.
27) F. Tuinstra and J. L. Koenig: J. Chem. Phys. **53** (1970) 1126.
28) R. J. Nemanich and S. A. Solin: Phys. Rev. B **20** (1979) 392.